DOI 10.24425/aee.2024.148861

Energy-saving optimal scheduling under multi-mode "source-network-load-storage" combined system in metro station based on modified Gray Wolf Algorithm

JINGJING TIAN[1], YU QIAN[1]✉, FENG ZHAO[1,2], SHENGLIN MO[1], HUAXUAN XIAO[1], XIAOTONG ZHU[1], GUANGDI LIU[1]

[1] *School of Automation and Electrical Engineering, Lanzhou Jiaotong University Lanzhou, China*

[2] *Key Laboratory of Opto-Technology and Intelligent Control Ministry of Education Lanzhou, China*

e-mail: ✉ *1095133417@qq.com*

(Received: 29.10.2023, revised: 01.03.2024)

Abstract: Aiming to address power consumption issues of various equipment in metro stations and the inefficiency of peak shaving and valley filling in the power supply system, this study presents an economic optimization scheduling method for the multi-modal "source-network-load-storage" system in metro stations. The proposed method, called the Improved Gray Wolf Optimization Algorithm (IGWO), utilizes objective evaluation criteria to achieve economic optimization. First, construct a mathematical model of the "source-network-load-storage" joint system with the metro station at its core. This model should consider the electricity consumption within the station. Secondly, a two-layer optimal scheduling model is established, with the upper model aiming to optimize peak elimination and valley filling, and the lower model aiming to minimize electricity consumption costs within a scheduling cycle. Finally, this paper introduces the IGWO optimization approach, which utilizes meta-models and the Improved Gray Wolf Optimization Algorithm to address the nonlinearity and computational complexity of the two-layer model. The analysis shows that the proposed model and algorithm can improve the solution speed and minimize the cost of electricity used by about 5.5% to 8.7% on the one hand, and on the other hand, it improves the solution accuracy, and at the same time effectively realizes the peak shaving and valley filling, which provides a proof of the effectiveness and feasibility of the new method.

Key words: bi-level optimization, Grey Wolf Optimization Algorithm, multi-mode, peak shaving and valley filling, source-network -load-storage

1. Introduction

Metro stations have become a crucial part of people's daily lives due to the significant rise in urban population, an emphasis on low carbon emissions, and environmental conservation. Consequently, singular form transport has made immense strides, with the Shanghai Metro serving as a prime example. For over 30 years, the Shanghai Metro has expanded exponentially, with 20 operating lines, 508 stations, and a total operating distance of 831 km, up from 1 line, 5 stations, and 6.6 km. The Shanghai Metro network remains the world's largest by size. An extra development phase began during the "14th Five-Year Plan" with plans to construct over 248 km and over 130 stations. Once all projects are complete, Shanghai Metro will boast 640+ stations with an operating mileage exceeding 1000 km, forming the world's inaugural cross-city rail transit system and linking Suzhou, Kunshan, and Shanghai concurrently. This plan furthers its influence by launching the first urban rail transit line that traverses provincial boundaries.

As is commonly known, metro stations and their trains require a substantial amount of electricity for power. The power consumed by a metro station is divided into two main categories: the first includes the power used for lighting, ticket gates, vending machines, and other electrical equipment, while the second is for heating and cooling systems used to regulate the station's temperature during the summer and winter. One of the main reasons for the low economic efficiency of metro operations is the substantial energy consumption, which represents a significant portion of the overall costs [1].

References [2–6] introduced the mathematical model of a PV power generation system, as well as the specific application of the PV power generation system connected with rail transit and the impact on power quality. Reference [2] introduced a model of a PV power generation system, which is similar to the mathematical model of a PV power generation system for urban rail transit. References [3,4] suggested the main ways of accessing PV. References [5,6] suggested the impact of grid-connected PV power systems. However, the current major researches are focused on electrified railroad systems, and fewer on urban rail transit systems. Urban rail transit systems are ideal for installing distributed photovoltaic power generation systems because they have vehicle bases, elevated stations, elevated intervals, parking lots, and vehicle maintenance and security bases, which are rich in light resources. Urban rail transit systems in the elevated station have a trellis roof interval noise barrier, vehicle base operation depot, maintenance depot and other building facilities away from the center of the building and no shade influence, the building area is relatively large, with the installation of photovoltaic modules of the basic conditions. Therefore, the urban rail transit system has superior light resource conditions, a sufficient installation area, better local consumption capacity and convenient grid connection conditions, and very suitable access to a PV power generation system. Therefore, it is feasible to connect the PV power generation system to the urban rail system, but it is necessary to consider its impact on the fluctuation of the power grid. References [7–10] proposed several different types of energy storage and scheduling methods. References [7,8] proposed the use of a single battery for energy storage, which is not only expensive but also has a short lifespan and a large cost of use, although the structure is simple and easy to realize. References [9,10] described a hybrid energy storage system consisting of a battery and a supercapacitor, which can achieve the optimal effect of peak shaving and valley filling while minimizing the cost of electricity consumption by using appropriate scheduling

methods. Therefore, incorporating solar and other new energy systems into the urban rail transit power supply system can reduce operating costs, while the use of hybrid energy storage systems can reduce the impact of their grid integration on the stability of the power grid.

In order to solve the problem of economy, on the one hand, it is necessary to establish the corresponding "source-net-charge-storage" joint system mathematical model, on the other hand, it is necessary to adopt reasonable energy management strategy. The first part "source" refers to the photovoltaic power generation system; the second part "grid" refers to the electric power grid; the third part "load" includes the electric cooling/heating system and all kinds of electric equipment in the subway station to maintain the appropriate temperature; the fourth part "storage" includes the hybrid energy storage system composed of supercapacitors and storage batteries [11]. References [12–14] proposed a daily scheduling and operation scheme of a "source-network-vehicle-storage" collaborative energy supply system for electrified railroads, which reduces the daily operation cost of substations, improves the regenerative braking energy and renewable energy capacity of electrified railroads, and realizes the win-win situation of environmental friendliness and economy. References [12, 13] proposed a mathematical model of "source-network-vehicle-storage" and developed the operation scheme. Reference [14] proposed a two-layer optimization model, which can improve the efficiency of model solving. For energy management strategies, References [15–20] proposed various energy management strategies and optimal scheduling schemes with economy and environmental protection as the main objectives. References [15, 16] proposed energy management strategies that aim at economic optimization, but they are basically single-objective oriented. References [17, 18] proposed energy management strategies for multi-modal, but there is a lack of energy management strategies and optimal scheduling methods with urban rail transit as the research background. References [19, 20] proposed energy management strategies under multi-objective, but no corresponding solution is proposed for the problem of slower model nonlinear solving. So, it is necessary to develop a rational energy management strategy and improve the solution methods based on the literature and the characteristics of urban rail transit.

Aiming at the power consumption of metro stations and the lack of economic peak shaving and valley filling in the power supply system, this paper proposes to take the photovoltaic, energy storage and power grid as the source, and the power required for the temperature regulation of the air conditioning system of a metro station in the winter and summer as the load so as to form a common power supply system with the metro station as the core of the "source-network-load-storage" system. Under the premise of ensuring the optimal effect of peak shaving and valley filling in the system, an optimization algorithm is used to find out the operation mode with the lowest cost of power consumption in the metro station.

2. Mathematical modeling of the "source-network-load-storage" combined power supply system

The photovoltaic power generation system and hybrid energy storage system are connected to the AC400V low-voltage distribution system side of the metro station, constituting a "source-network-load-storage" joint system as shown in Fig. 1.

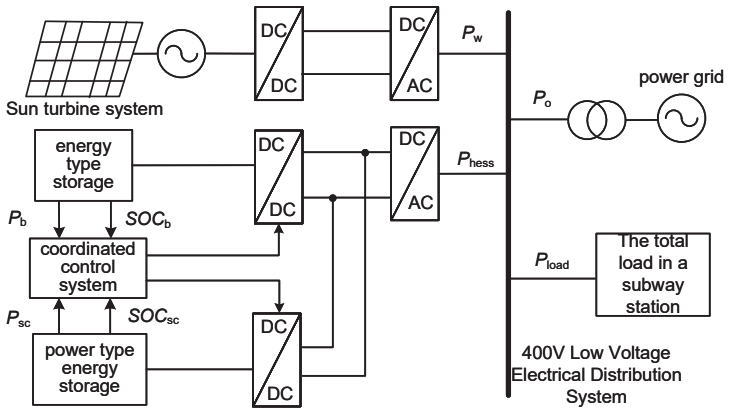

Fig. 1. Structure of source-network-load-storage system

2.1. Mathematical modeling of photovoltaic power generation systems

The PV cell output power expression is:

$$P_{\mathrm{V}}(t) = P_{\mathrm{STC}} \times \frac{S_{\mathrm{ref}}\left[1 + k\left(T_{\mathrm{C}} - T_{\mathrm{R}}\right)\right]}{S_{\mathrm{STC}}}. \tag{1}$$

In Formula (1): $P_{\mathrm{V}}(t)$ is the PV output power at time t; P_{STC} stands for the standard conditions of the maximum test power; S_{STC} stands for the standard test conditions of the maximum light intensity; S_{ref} represents the standard test conditions of the light intensity; T_{C} applies to the standard test conditions of the ambient temperature; T_{R} stands for the standard conditions of the reference temperature; k is the power temperature coefficient.

2.2. Hybrid energy storage system modeling

Hybrid energy storage systems contain both battery and super-capacitor components. Adopting a hybrid energy storage system achieves better peak shaving and valley filling than single energy storage, mainly by using a power allocation method for system capacity allocation.

The expression of hybrid energy storage SOC is:

$$\begin{cases} \mathrm{SOC_b}(t) = \mathrm{SOC_b}(t-1) + \dfrac{\gamma \displaystyle\int P(t)\mathrm{d}t}{E} \times 100\% \\ \mathrm{SOC_{SC}}(t) = \dfrac{U(t) - U_{\mathrm{CMIN}}}{U_{\mathrm{CMAX}} - U_{\mathrm{CMIN}}} \end{cases}. \tag{2}$$

In Formula (2), $\mathrm{SOC_b}(t)$ is the remaining capacity of the battery at the moment of t; $P(t)$ is the power of energy storage charging and discharging at the moment of t, which is positive in the charging state and negative in the discharging state; E is the rated capacity of the battery; is the efficiency value of the charging and discharging of the energy storage system; $\mathrm{SOC_b}(t-1)$ is the remaining capacity of the battery at the moment of $t-1$; $\mathrm{SOC_{SC}}$ is the SOC of the super-capacitor; $U(t)$ is the voltage of the super-capacitor at the moment of t; U_{CMAX} is the maximum of the terminal voltage; U_{CMIN} is the minimum value of the terminal voltage.

2.3. Mathematical modeling of electric heating/cooling

The power output expression for electric heating/cooling is [21, 23]:

$$q = P_{\mathrm{AIR}} \times F_{\mathrm{STA}} \times S_{\mathrm{STA}}, \tag{3}$$

$$Q(t) = V_{\mathrm{AIR}} \times q \times |T_{\mathrm{IN}} - T_{\mathrm{OUT}}(t)|, \tag{4}$$

$$P_{\mathrm{k}}(t) = \begin{cases} \dfrac{Q(t)}{\mathrm{EER_{RE}}} & \text{Heating} \\ \dfrac{Q(t)}{\mathrm{EER_{LE}}} & \text{Cooling} \end{cases}. \tag{5}$$

In Formula (3), q is the total mass of air in a metro station; F_{STA} is the standard ventilation volume in a metro station; S_{STA} is the total area of a metro station.

In Formula (4), $Q(t)$ is the cooling/heating load consumed at time t to ensure that the required temperature is maintained in the metro station; V_{AIR} is the specific heat capacity of the air in the metro station; T_{IN} is the standard temperature required in the metro station; $T_{\mathrm{OUT}}(t)$ is the ambient temperature outside the metro station at time t.

In Formula (5), $P_{\mathrm{k}}(t)$ is the electric power consumed by the electric heating/cooling system at time t; $\mathrm{EER_{RE}}$ is the energy efficiency ratio of the electric heating system; $\mathrm{EER_{LE}}$ is the energy efficiency ratio of the electric cooling system.

2.4. Heat dissipation electrical equipment in metro stations

Metro stations contain a significant amount of electrical equipment. The operation of these devices not only consumes electricity but also generates heat. The electrical equipment can be divided into two categories: the Metro Station Public Area Equipment and the Metro Station Equipment Area Equipment. Table 1 illustrates heat dissipation of electrical equipment in the Metro Station Public Area, while Table 2 displays heat dissipation of equipment in the Metro Station Equipment Area. Technical terms will be explained when they are first utilized. "Tai/kW" means the amount of heat dissipated per hour per piece of equipment.

Table 1. Equipment in public areas of metro stations

Title	Dissipation of heat	Title	Dissipation of heat
Automatic Vending Machine	0.3 (Tai/kW)	Lighting Equipment	20 (Tai/kW)
Turnstile	0.2 (Tai/kW)	Communications Equipment	2.5 (Tai/kW)
Ticket Machines at the Box Office	0.3 (Tai/kW)	Barrier-free Elevators	6.5 (Tai/kW)
Escalator	4.5 (Tai/kW)	Safety Equipment Room	5 kW
Station Control Rooms	5 kW	Public Safety Equipment Room	8 kW

Continued on next page

Table 1 – *Continued from previous page*

Title	Dissipation of heat	Title	Dissipation of heat
Communication Power Supply Room	10 kW	Surveillance Equipment Room	15 kW
Communication Equipment Room	20 kW	Other Heat Dissipation Equipment	150 (Tai/kW)

Table 2. Metro Station Equipment Area

Title	Dissipation of heat	Title	Dissipation of heat
AFC Ballot Box Office	2 kW	1500 V DC Switchgear Cabinet	35 kW
AFC Equipment Rooms	5 kW	35 kV Switchgear Compartment	14 kW
Signal Power Supply Room	10 kW	400 V Switchgear Compartment	55 kW
Signal Equipment Rooms	20 kW	Battery Compartment	5 kW
Electronic Control Room for Environmental Control	19 kW	Rectifier Transformer Room	36 kW
Lighting Distribution Rooms	3 kW	Renewable Energy Installation Room	27 kW

Some of the equipment in the metro station will also emit a certain amount of heat while using electricity, which plays a different role in different seasons. In the winter, the heat emitted by the electric equipment will offset part of the heat load required to maintain the appropriate temperature in the metro station, thus reducing the output of the electric heating system; in the summer, the heat emitted by the electric equipment will increase part of the cold load required to maintain the appropriate temperature in the metro station, thus increasing the output of the electric cooling system.

3. Constraints and objective functions

Due to the implementation of photovoltaic technology, the stability of the existing power supply system may be affected. To address this, a hybrid energy storage system can be integrated into the "source-network-load-storage" joint system. This will ensure system stability while also improving the overall economic efficiency of the system. The hybrid energy storage system utilized for grid shaving should consider economic factors. Selecting the appropriate energy storage capacity during the corresponding period is crucial in maximizing peak shaving or filling the valley. This will avoid redundancy and, at the same time, adhere to power grid requirements, decreasing network load loss.

This paper uses a 24-hour scheduling cycle to address the peak shaving and valley filling scheduling problem in hybrid energy storage systems. The objective function selected is to optimize peak shaving and valley filling for enhanced grid stability while minimizing electricity

consumption costs. Considering the determination of the scheduling strategy and operation state for the hybrid energy storage system, the solution process is divided into two layers. The optimal two-layer scheduling structure is depicted in Fig. 2.

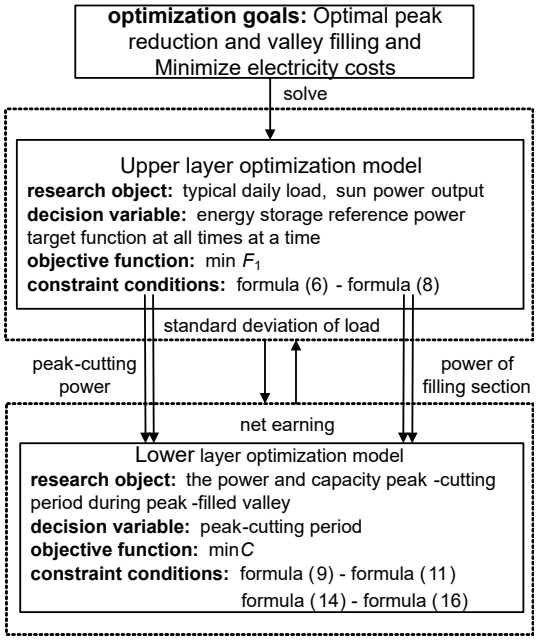

Fig. 2. Structure of bi-level optimized scheduling for peak load shifting with energy storage system

3.1. Objective function

The objective function comprises two components: optimizing the peak and valley elimination effect of the integrated "source-network-load-storage" system and minimizing the cost of electricity consumption.

1) Objective function

① Optimized peak and valley cancellation

Factors such as power load demand and uncertainty with electricity load make it difficult for the power grid to run smoothly, and it is necessary to achieve effective balance through energy storage technology. If the load demand is low at a time, the mixed energy storage system can store part of the energy; if the load demand is high at a certain time, part of the energy is released. Therefore, the upper-layer optimization model uses an equivalent load standard deviation to measure the steady effect of the peak-cutting valley. The smaller the peak valley, the larger the peak coefficient, as shown in Formula (6):

$$\min F_1 = \sqrt{\frac{1}{T}\sum_{t=1}^{T}(P_t - P_{\text{av}})^2}. \tag{6}$$

Combined system net load power balance, as shown in Formula (7):

$$P_t = P_{\text{load}} - P_{\text{w}} + P_{\text{hess}}. \tag{7}$$

Solving for the average net load power, as shown in Formula (8):

$$P_{\text{av}} = \frac{1}{T}\sum_{t=1}^{T} P_t. \tag{8}$$

In Formula (7), P_t is the net load power of the system at the time of t; P_{load} is the power of the load at the time of t; P_{V} is the output power of the sun; P_{hess} is the reference power of the hybrid energy storage system; when $P_{\text{hess}} > 0$ indicates the discharge of the energy storage system, $P_{\text{hess}} < 0$ means the energy storage system is charged.

In Formula (8), P_{av} is the average value of the net load.

(2) Minimize electricity costs

In order to ensure the normal operation of the "source-network-charge-storage" joint system, the cost of electricity mainly includes the maintenance cost of the photovoltaic power generation system, the interaction cost with the grid, and the profit of the hybrid energy storage system to store and release the energy in the valley and the usual tariff period, if the energy is released in the peak tariff period, the difference between the peak and the valley tariffs will be the profit, and if the energy is released in the usual tariff period, the difference between the valley and the flat tariffs will be the profit.

The peak-to-valley tariff for an area is shown in Fig. 3.

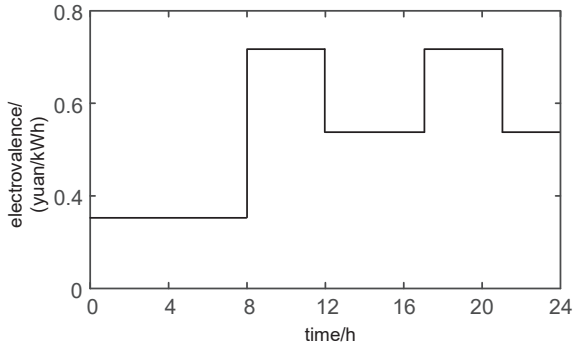

Fig. 3. Peak-valley time-sharing electricity price map of a region

The cost of electricity consumption in a dispatch cycle (24 h) can be expressed as:

$$\min C = C_{\text{V}} + C_{\text{SOC}} + C_{\text{D}}. \tag{9}$$

In Formula (9), C_{V} is the maintenance cost of the PV unit; C_{D} is the profit of interaction between the system and the grid; C_{SOC} is the operating cost of the hybrid energy storage system.

The cost of interaction with the grid can be expressed as:

$$C_{\text{D}} = \begin{cases} P_{\text{D}} \times C_{\text{FEI}} & C_{\text{FEI}} \le 0 \\ P_{\text{D}} \times C_{\text{FFI}} & C_{\text{FEI}} \ge 0 \end{cases}. \tag{10}$$

In Formula (10), P_{D} is the grid interaction power; C_{FEI} is the cost of interacting with the grid at different moments.

$$\begin{cases} C_{\mathrm{SOC}} = C_t + C_{\mathrm{iv}} + C_{\mathrm{ivb}} + C_{\mathrm{ivsc}} + C_{\mathrm{omc}} + C_{\mathrm{dc}} \\ C_t = C_{\mathrm{iv}} + C_{\mathrm{omc}} + C_{\mathrm{dc}} \\ C_{\mathrm{iv}} = C_{\mathrm{ivb}} + C_{\mathrm{ivsc}} \\ C_{\mathrm{ivb}} = (C_{\mathrm{bp}} P_{\mathrm{b}} + C_{\mathrm{be}} E_{\mathrm{b}}) \dfrac{\varepsilon(1+\varepsilon)^{L_{\mathrm{b}}}}{(1+\varepsilon)^{L_{\mathrm{b}}} - 1} \\ C_{\mathrm{ivsc}} = (C_{\mathrm{scp}} P_{\mathrm{sc}} + C_{\mathrm{sce}} E_{\mathrm{sc}}) \dfrac{\varepsilon(1+\varepsilon)^{L_{\mathrm{sc}}}}{(1+\varepsilon)^{L_{\mathrm{sc}}} - 1} \\ C_{\mathrm{omc}} = C_{\mathrm{bom}} E_{\mathrm{b}} + C_{\mathrm{scom}} E_{\mathrm{sc}} \\ C_{\mathrm{dc}} = C_{\mathrm{dcb}} E_{\mathrm{b}} + C_{\mathrm{dcsc}} E_{\mathrm{sc}} \end{cases} . \tag{11}$$

In Formula (11), C_{bp}, C_{be} are the unit power cost and unit capacity cost of the battery; C_{scp}, C_{sce} are the unit power cost and unit capacity cost of the super-capacitor; C_{ivb} is the investment cost of the battery; C_{ivsc} is the investment cost of the super-capacitor; L_{b} is the service life of the battery; L_{sc} is the service life of the super-capacitor; ε is the discount rate; C_{bom}, C_{dcb} are the operation and maintenance cost of the battery and the cost of the super-capacitor; C_{scom}, C_{dcsc} represent the operation, maintenance cost and the cost of the super-capacitor as well as the cost of the disposal of the super-capacitor.

3.2. Primary section 2 voltage stabilization control strategy

The constraints of the combined "source-network-load-storage" system are mainly composed of two parts, which are the electric load balance and the operation constraints of different micro-sources.

1) Power grid power balance constraint

When the hybrid energy storage system is in a discharged state:

$$P_{\mathrm{k}} + P_{\mathrm{STA}} = P_{\mathrm{D}} + P_{\mathrm{V}} + P_{\mathrm{SOC,OUT}} \eta_{\mathrm{OUT}}. \tag{12}$$

In Formula (12), P_{STA} is the electric power consumed by the electric equipment in the metro station; $P_{\mathrm{SOC,OUT}}$ is the power when the hybrid energy storage system is discharged; η_{OUT} is the discharge efficiency of the hybrid energy storage system.

When the hybrid energy storage system is in a state of charge:

$$P_{\mathrm{k}} + P_{\mathrm{STA}} + \frac{P_{\mathrm{SOC,IN}}}{\eta_{\mathrm{IN}}} = P_{\mathrm{D}} + P_{\mathrm{V}}. \tag{13}$$

In Formula (13), η_{IN} is the efficiency of the hybrid energy storage system when discharging; $P_{\mathrm{SOC,IN}}$ is the power of the hybrid energy storage system when charging.

2) Constraint condition for different micro sources

The operational constraints of different micro sources contain PV power constraints, hybrid storage system SOC constraints, and power constraints for interaction with the grid.

Optimized peak and valley cancellation

$$P_{\mathrm{V,MIN}} \le P_{\mathrm{V}} \le P_{\mathrm{V,MAX}}. \tag{14}$$

In Formula (14), $P_{V,MIN}$ is the lower power limit of PV power generation; $P_{V,MAX}$ is the upper power limit of PV power generation.

Energy storage SOC constraint

To ensure that the energy storage system is running within the scope of safety, its battery and super-capacitors SOC should be controlled at the upper and lower limit, that is:

$$\begin{cases} SOC_{L\text{-}b} \le SOC_b(t) \le SOC_{U\text{-}b} \\ SOC_{L\text{-}sc} \le SOC_{sc}(t) \le SOC_{U\text{-}sc} \end{cases}. \tag{15}$$

In Formula (15), $SOC_{L\text{-}b}$, $SOC_{U\text{-}b}$ are the upper and lower limits of the SOC of the battery; $SOC_{L\text{-}sc}$, $SOC_{U\text{-}sc}$ are the upper and lower limits of the SOC of the super-capacitor, respectively.

Power constraints for interaction with the grid

$$P_{D,MIN} \le P_D \le P_{D,MAX}. \tag{16}$$

In Formula (16), $P_{D,MIN}$ is the lower limit of power interacting with the grid; $P_{D,MAX}$ is the upper limit of power interacting with the grid.

4. Solving algorithm

In this paper, a combination of the meta model and the improved Gray Wolf Optimization (IGWO) Algorithm is used to solve the developed model.

4.1. Metaphysical method

The meta model is usually called the response surface. It refers to the function relationship between output variables and a set of input variables. For the current computing process and optimization goals (such as multi-field simulation, FEA, CFD, etc.) models, the meta model can be used as a simple model, that is, the model of model. Therefore, the meta model is also known as the proxy model, that is, the original complex model that replaces expensive costs to improve the solution efficiency. Figure 4 shows the principle of the metaphysical model method.

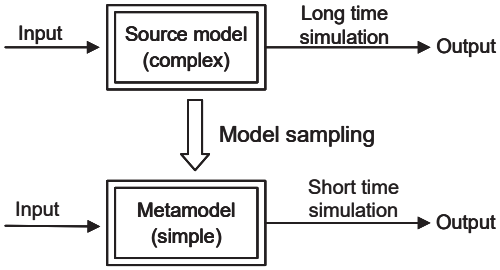

Fig. 4. Principle of meta model method

4.2. The improved Gray Wolf Optimization Algorithm (IGWO) combined with Lévy flight

The Gray Wolf Optimization (GWO) Algorithm is a stochastic metaheuristic algorithm designed to optimize through emulation of the cooperative behavior and social hierarchy of gray wolf packs, which mirrors their predatory instincts.

The GWO algorithm has several advantages such as its simple structure, few adjustable parameters, and ease of implementation. It also includes an adaptable convergence factor and information feedback mechanism, which enables a dynamic balance between local optimization and global search. These features result in superior accuracy and faster convergence when addressing problems.

The Gray Wolf Algorithm's focus is on emulating the hunting actions of gray wolf packs within natural settings. The algorithm comprises four fundamental steps:

1. Initialization: The problem that needs optimizing is converted into one or more objective functions and constraints, and an initial population is created by generating a group of individuals randomly.
2. Finding prey: based on objective evaluations of individuals' performance in identifying the optimal solution of the objective function, the three individuals with the best performance are identified as the leader wolf, also known as the head wolf: -wolf, -wolf, and -wolf.
3. Adjust position: utilize the alpha wolf's position to communicate a message to the other wolves, informing them of the alpha's location and directing them to move towards.
4. Updating parameters: update the search parameters and capabilities of gray wolves of different ranks based on the gray wolf packs rank ranking [24].

A Lévy flight, named after French mathematician Paul Lévy, describes a form of random walk in which the step length probability distribution is heavy-tailed. This distribution indicates a higher likelihood of taking a large stride during the random walk process. Compared to the random walk with a step size distribution without heavy tails, the motion trajectory of a Lévy flight is more random. Adding a Lévy flight to the algorithm can effectively reduce the probability of the original algorithm falling into a partial optimum.

The algorithm effectively avoids falling into local optimal solutions and increases the probability of finding the global optimal solution. It does this by combining a Lévy flight with the multi-objective Gray Wolf Algorithm.

4.3. "Source-network-load-storage" joint operation scheduling optimization

Because the seasons differ, the metro station requires varying loads to maintain indoor temperature. During the winter, the station requires a significant amount of heat load to raise the temperature, while during the summer, it requires a cold load to lower the temperature. During the spring and autumn, the temperature in the metro station is similar to the ambient temperature, necessitating minimal additional heat and cold loads. Therefore, optimizing the operation and scheduling of the "source-network-load-storage" combined system for a metro station can be divided into three phases.

The metro station typically operates from 6 a.m. to 12 p.m. During other periods, a limited number of staff remain at the station for daily maintenance and repair. However, due to the insufficient staff, the heating and cooling load may not be provided during these times. Table 3

displays the optimized schedule for varying seasons, and the table employs the partial electrical load balance equation.

The operating hours of the metro station are usually from 6 a.m. to 0 p.m. The other times may leave a few staff in the ground body station for daily maintenance and repair, but due to the low number of employees, this period may not be enough to provide the cooling and heating load. The optimized scheduling for different seasons is shown in Table 3, and the partial electrical load balance equation used in the table is as follows.

$$P_{\mathrm{STA}} + \frac{P_{\mathrm{SOC,IN}}}{\eta_{\mathrm{IN}}} = P_{\mathrm{D}}, \tag{17}$$

$$P_{\mathrm{k}} + P_{\mathrm{STA}} = P_{\mathrm{D}} + P_{\mathrm{SOC,OUT}}\eta_{\mathrm{OUT}}, \tag{18}$$

$$P_{\mathrm{k}} + P_{\mathrm{STA}} + \frac{P_{\mathrm{SOC,IN}}}{\eta_{\mathrm{IN}}} = P_{\mathrm{D}}, \tag{19}$$

$$P_{\mathrm{STA}} = P_{\mathrm{D}} + P_{\mathrm{V}} + P_{\mathrm{SOC,OUT}}\eta_{\mathrm{OUT}}, \tag{20}$$

$$P_{\mathrm{STA}} + \frac{P_{\mathrm{SOC,IN}}}{\eta_{\mathrm{IN}}} = P_{\mathrm{D}} + P_{\mathrm{V}}, \tag{21}$$

$$P_{\mathrm{STA}} + \frac{P_{\mathrm{SOC,IN}}}{\eta_{\mathrm{IN}}} = P_{\mathrm{D}}, \tag{22}$$

$$P_{\mathrm{STA}} = P_{\mathrm{D}} + P_{\mathrm{SOC,OUT}}\eta_{\mathrm{OUT}}. \tag{23}$$

In the table, Mode I above prioritizes power supply to the grid, followed by the hybrid energy storage system; Model II prioritizes power supply for the PV system, followed by the grid and finally the hybrid energy storage system; Model III prioritizes power supply for the PV system,

Table 3. Optimal scheduling in different seasons

Season	**Time**	**Metro station whether running**	**Is the sun rising**	**Types of tariffs**	**Required load type**	**Power mode**	**Electric load balance**
Winter	0–6	No	No	Valley times	Not have	Mode I	Formula (17)
	6–8	Yes	Yes		Heat load	Mode II	Formula (13)
	8–12			Peak times		Mode III	Formula (12)
	12–16			Normal times		Mode IV	Formulas (12), (13)
	16–18			Peak times		Mode III	Formula (12)
	18–20		No			Mode V	Formula (18)
	20–0			Normal times		Mode VI	Formulas (18), (19)

Continued on next page

Table 3 – *Continued from previous page*

Season	**Time**	**Metro station whether running**	**Is the sun rising**	**Types of tariffs**	**Required load type**	**Power mode**	**Electric load balance**
Summer	0–6	No	No	Valley times	Not have	Mode I	Formula (17)
	6–8	Yes	Yes		Cold load	Mode II	Formula (13)
	8–12			Peak times		Mode III	Formula (12)
	12–16			Normal times		Mode IV	Formulas (12), (13)
	16–18			Peak times		Mode III	Formula (12)
	18–20		No			Mode V	Formula (18)
	20–0			Normal times		Mode VI	Formulas (18), (19)
Spring and autumn	0–6	No	No	Valley times	Not Have	Mode I	Formula (17)
	6–8	Yes	Yes			Mode II	Formula (21)
	8–12			Peak times		Mode III	Formula (20)
	12–16			Normal times		Mode IV	Formulas (21), (20)
	16–18			Peak times		Mode III	Formula (20)
	18–20		No			Mode V	Formula (23)
	20–0			Normal times		Mode VI	Formulas (22), (23)

followed by the hybrid energy storage system and finally the grid; Mode IV prioritizes power supply for the PV system, followed by the interaction of the grid and the hybrid energy storage system for power supply; Mode V prioritizes power supply for hybrid energy storage systems, followed by the grid; Mode VI is a hybrid energy storage system and grid interaction for power supply.

5. Analysis of example

In this paper, the real output power of a photovoltaic farm with a 25 MW installed capacity located in the metro station is utilized as sample data for a typical day spanning 24 hours, as illustrated in Fig. 5.

Since metro stations are usually built underground, there are special factors such as geothermal heat, and there is no need to activate the electric cooling or heating system in the spring and fall to maintain the appropriate temperature in the metro station, which has a negligible impact on the operating cost of the metro station, so the analysis of the example is performed only for the winter and summer, and the average temperatures of the hottest month and the coldest month of the year are selected as the variables to be analyzed and calculated.

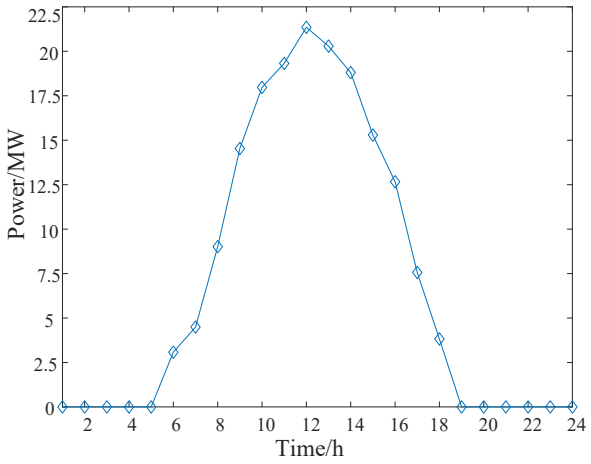

Fig. 5. Reference power curve for photovoltaic generation

5.1. Analysis of winter arithmetic examples

The main source of energy consumption in the "source-network-load-storage" system is electric heating. In the winter, when temperatures drop, the metro station requires a significant amount of heat to maintain standard temperatures.

Under the condition of ensuring the optimal effect of system peak shaving and valley filling and minimizing the cost of electricity, the performance of different micro-sources in the winter is shown in Fig. 6. As the light intensity, temperature, and heat dissipation of the electrical equipment

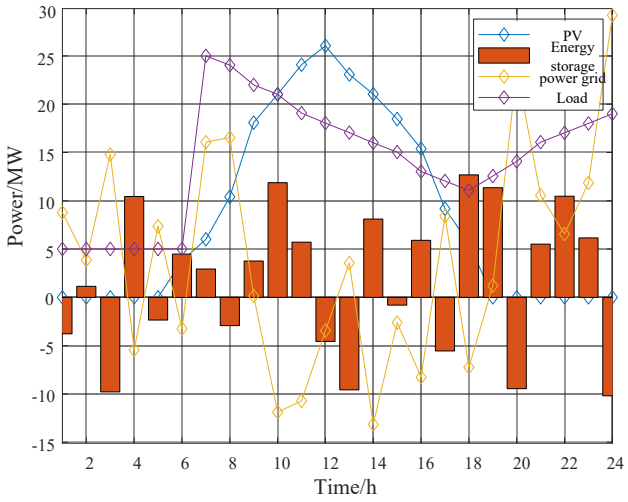

Fig. 6. Winter output power of different micro sources

in the station increase, while the passenger flow decreases, the total load decreases, and there may be a situation where the PV power generation exceeds the compliance.

The output of a hybrid energy storage system in a combined "source-network-load-storage" system in the winter is shown in Fig. 7.

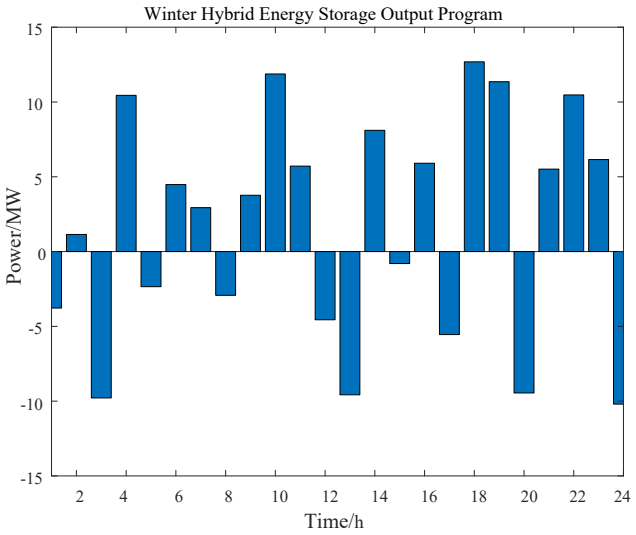

Fig. 7. Winter output power of hybrid energy storage system

The output of the grid in a combined "source-network-load-storage" system in the winter is shown in Fig. 8.

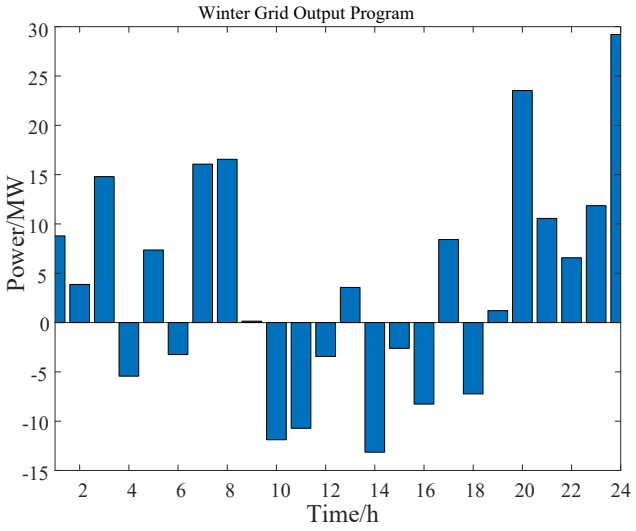

Fig. 8. Power output of winter power grid

The variation of the required heat load in the metro station at different moments of winter is shown in Fig. 9.

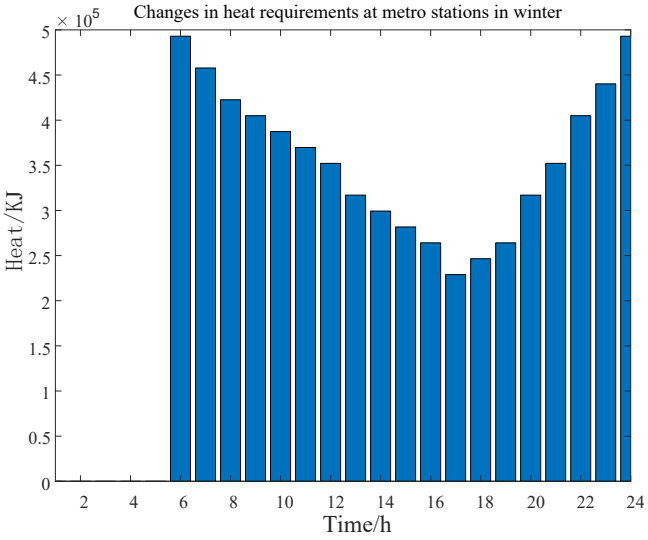

Fig. 9. Winter heat load variation of metro station

The variation of electric power consumed by an electric heating system in the metro station at different moments in the winter is shown in Fig. 10.

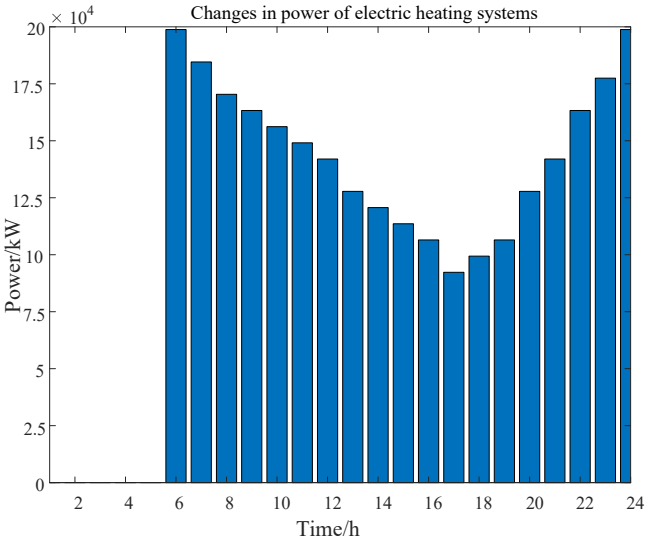

Fig. 10. Changes in electrical power of a metro station's electric heating system in the winter

5.2. Analysis of summer arithmetic examples

In the summer, high temperatures require significant cooling loads to maintain standard temperatures in metro stations. Electric refrigeration is the primary source of energy consumption in the "source-network-load-storage" system.

Under the condition of ensuring the optimal effect of system peak shaving and valley filling and minimizing the cost of electricity, the performance of different micro-sources in the summer is shown in Fig. 11.

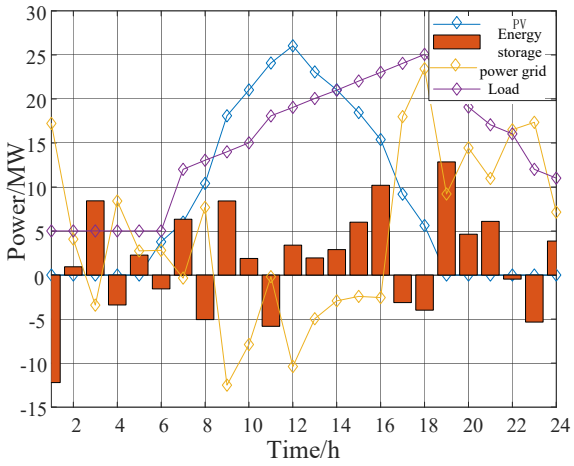

Fig. 11. Summer output power of different micro source

The output of a hybrid energy storage system in a combined "source-network-load-storage" system in the summer is shown in Fig. 12.

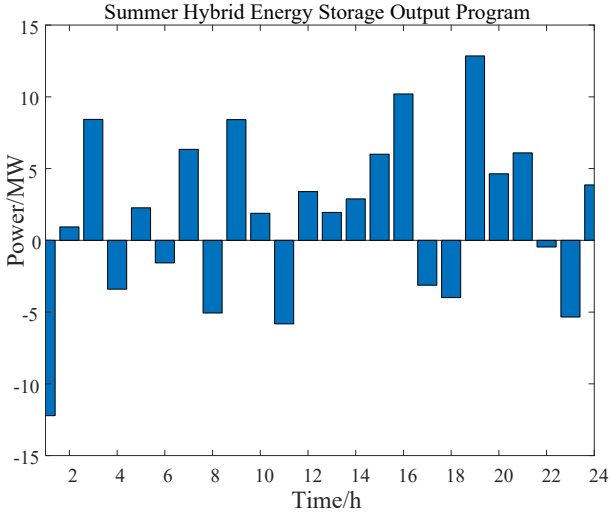

Fig. 12. Summer output power of hybrid energy storage system

The output of the grid in a combined "source-network-load-storage" system in the summer is shown in Fig. 13.

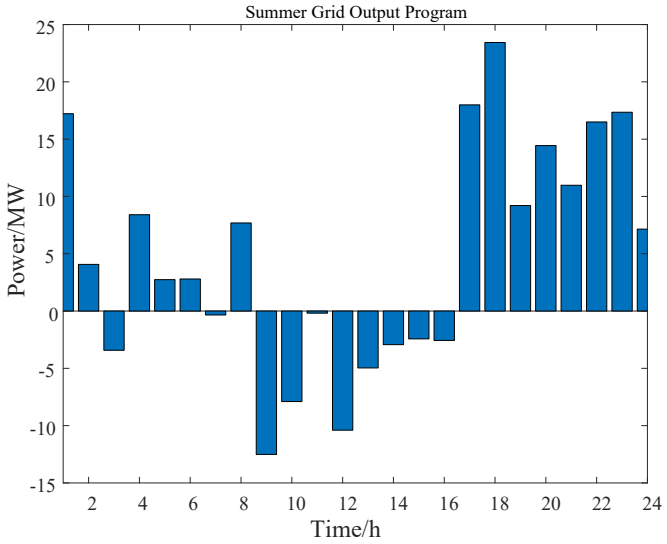

Fig. 13. Power output of summer power grid

The variation of the required cooling load in the metro station at different moments in the summer is shown in Fig. 14.

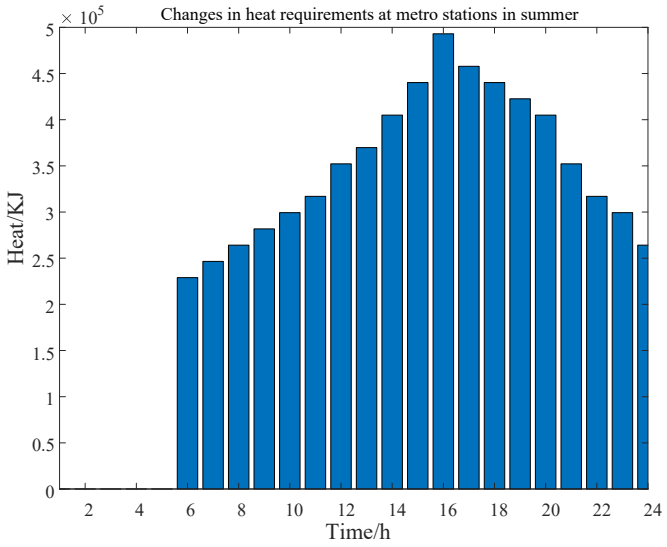

Fig. 14. Changes in cooling load of a metro station in the summer

The variation of the electric power consumed by the electric refrigeration system in the metro station at different moments in the summer is shown in Fig. 15.

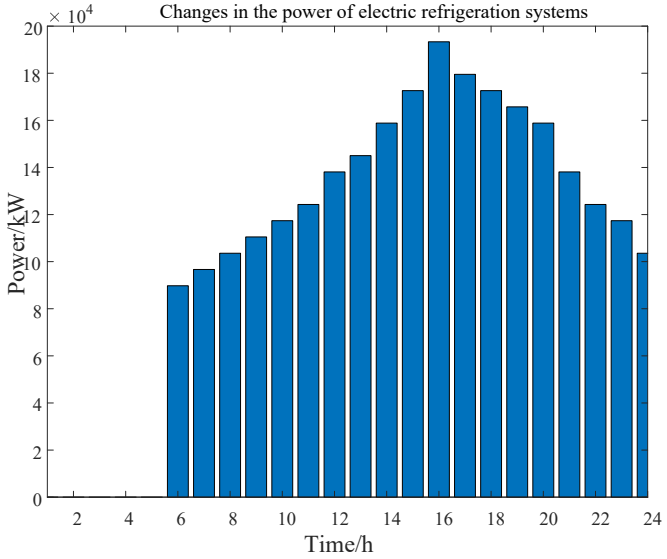

Fig. 15. Changes in electric cooling power of a metro station in the summer

5.3. Algorithm comparison analysis

The restricted diversity within the population of the Gray Wolf Optimization (GWO) algorithm arises from the initial population generation method utilized by the GWO algorithm. Random initialization is not a dependable technique for ensuring population diversity [25, 26]. Additionally, the GWO algorithm's search mechanism accounts for the issue of slower convergence in later stages.

Wolves mainly rely on the distance from the -wolf, -wolf, and -wolf, also known as the lead wolf, to assess the proximity between themselves and their prey. Unfortunately, this often leads to slower convergence in the later stages and increases the likelihood of getting stuck in local optima. This is because the position of the -wolf may not necessarily correspond to the global optimal solution. Moreover, the -wolf continuously approaches the lead wolf during the iterative process, causing the GWO algorithm to potentially fall into local optima. To address these issues, this paper proposes the following improvement method:

1) A Gaussian distribution is implemented to enhance the diversity of the gray wolf population. The enhanced initial population distribution is illustrated in Formula (24).

$$\begin{aligned} \gamma &= \text{rand}\, n(), \\ C &= 2 \times \gamma. \end{aligned} \tag{24}$$

2) The linear inertia weight factor is modified from linear to nonlinear to accelerate the convergence speed while enhancing the convergence accuracy [27, 28]. The upgraded inertia

weight factor is demonstrated in Formula (25).

$$\partial = 2\cos\left(\left(\frac{\frac{\pi}{2}}{\text{MaxIter}}\right)\times\left(\frac{k}{k_{\max}}\right)^4\right). \tag{25}$$

3) Levy flight is introduced to avoid the resulting results from falling into a local optimum.

To assess the performance of the IGWO algorithm proposed in this study, the standard GWO algorithm and the APSO (Adaptive Particle Swarm Optimization) algorithm will also be analyzed and compared. Consequently, appropriate parameters must be chosen based on the hybrid energy storage system, as shown in Table 4.

Table 4. Relative parameters of energy storage system

Object	**Performance index**	**Parameter**
Storage battery	Unit power cost/(yuan/kW)	2 700
	Unit capacity cost/(yuan/kWh)	640
	Operational and maintenance cost/(yuan/kWh)	0.05
	Cost of disposal/(yuan/kWh)	–0.04
	Charge discharge efficiency/%	80
	Bound of SOC/%	(20 80)
	Cycle service life/time	1 000
Super-capacitor	Unit power cost/(yuan/kW)	1 500
	Unit capacity cost/(yuan/kWh)	27 000
	Operational and maintenance cost/(yuan/kWh)	0.05
	Cost of disposal/(yuan/kWh)	–0.05
	Charge discharge efficiency/%	95
	Bound of SOC/%	(10 90)
	Operating life/y	20
Else	Discount rate/%	6

The three algorithms were executed sequentially 10 times and their computational outputs are displayed in Fig. 16.

After conducting 10 calculations of the three algorithms, it was found that the GWO, APSO, and IGWO have a minimum electricity cost of EUR 3757.61, EUR 3548.07, and EUR 3447.17, respectively. The GWO algorithm's cost is slightly higher compared to that of the APSO and IGWO algorithms, with an increase of 5.57% and 8.61%, respectively.

The performance comparison of three algorithms is available in Fig. 17. It is evident that the Improved GWO algorithm (IGWO) outperforms the other two in terms of both solution speed and accuracy. Therefore, the IGWO algorithm is advantageous in resolving global optimization models.

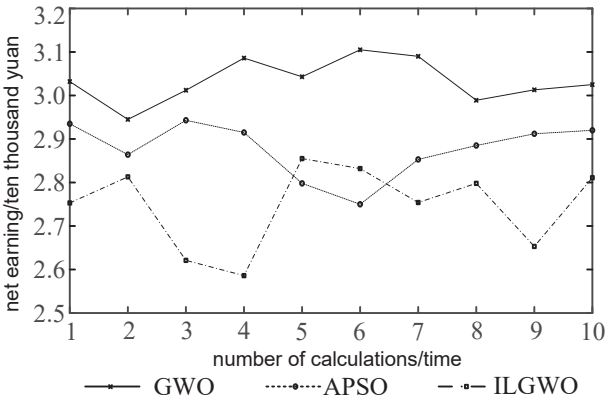

Fig. 16. Results after ten calculations of three algorithms

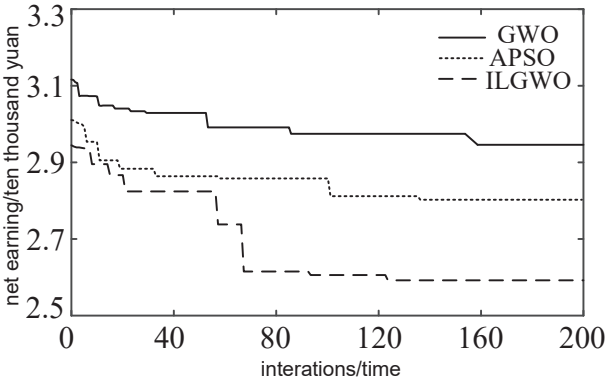

Fig. 17. Optimization performance comparison of three algorithm

6. Conclusions

This work presents a multi-objective optimization model for scheduling the energy consumption of a metro system over the course of the year, incorporating constraints for achieving optimal peaks and valleys, and minimizing the cost of power. Based on our analysis, we draw conclusions and provide examples to support our findings.

1. This paper presents a mathematical optimization model and constraints for the "source-network-load-storage" joint system, focusing on the metro station as the core. The model offers a theoretical foundation for achieving an economically efficient solution to energy consumption in metro stations during various seasons.
2. For the multi-objective model that optimizes a two-layer nonlinear system, the arithmetic analysis of this paper verifies the dual balance of the reliability of the energy storage system and the economic efficiency for peak shaving and valley filling.

3. In this paper, we use the combined "source-network-load-storage" system optimization model and an enhanced Grey Wolf Optimization algorithm (GWO) to address the challenge of reducing the cost of electricity consumption. Our results demonstrate that the enhanced GWO algorithm, aka the IGWO algorithm, outperforms the original algorithm in global searchability, convergence accuracy, and computational speed for this multi-objective optimization problem.

References

[1] Song Jie, Zheng Yi *et al.*, *Research on Performance Optimization of Ventilation and Air Conditioning Systems for Equipment Management Rooms in Subway Station Based on Actual Measurements*, Shanghai Energy Saving (in Chinese), no. 6, pp. 806–813 (2023).

[2] Xie Shaofeng, Fang Manqi, Xia Guohua, *Influence of PV generation system accessing to traction power supply system on power quality*, Electric Power Automation Equipment (in Chinese), vol. 38, no. 10, pp. 53–59 (2018).

[3] Chen Weirong, Wang Xuan, Li Qi *et al.*, *Review on the Development Status of PV Power Station Accessing to Traction Power Supply System for Rail Transit*, Power System Technology (in Chinese), vol. 43, no. 10, pp. 3663–3670 (2019).

[4] Tang Jie, Li Yiran, Huang Ruanyuan *et al.*, *Capacity Allocation off BESS in Secondary Frequency Regulation with the Goal of Maximum Net Benefit*, Transactions of China Electrotechnical Society (in Chinese), vol. 43, no. 8, pp. 3048–3059 (2023).

[5] Hu Haitao, Ge Yinbo, Huang Yi *et al.*, *"Source-network-train-storage" Integrated Power Supply System for Electric Railways*, Proceedings of the CSEF (in Chinese), vol. 42, no. 12, pp. 4374–4391 (2022).

[6] Andoni S., Aitor M., Haizea G. *et al.*, *Co-Optimization of Storage System Sizing and Control Strategy for Intelligent Photovoltaic Power Plants Market Integration*, IEEE transactions on sustainable energy, vol. 7, no. 4, pp. 1749–1761 (2016), DOI: 10.1109/TSTE.2016.2555704.

[7] Deng Wenli, Dai Zhaohua, Chen Weirong *et al.*, *Review on the Development Status of PV Power Station Accessing to Traction Power Supply System for Rail Transit*, Power System Technology (in Chinese), vol. 39, no. 19, pp. 5692–5702+5897 (2019).

[8] Loakimidis C., Thomas D., Rycerski P. *et al.*, *Peak shaving and valley filling of power consumption profile in non-residential buildings using an electric vehicle parking lot*, Energy, vol. 148, pp. 148–158 (2018), DOI: 10.1016/j.energy.2018.01.128.

[9] Garcia-Plaza M., Eloy-Garcia Carrascoet J., Alonso-Martinez J. *et al.*, *Peak shaving algorithm with dynamic minimum voltage tracking for battery storage systems in microgrid applications*, Journal of Energy Storage, vol. 20, pp. 41–48 (2018), DOI: org/10.1016/j.est.2018.08.021

[10] Li Junhui, Zhang Jiahui, Mu Gang *et al.*, *Day-ahead optimal scheduling strategy of peak regulation for energy storage considering peak and valley characteristics of load*, Electric Power Automation Equipment (in Chinese), vol. 40, no. 7, pp. 128–133+140+134–136 (2020).

[11] Hu Haitao, Zheng Zheng, He Youzheng *et al.*, *The Framework and Key Technologies of Traffic Energy Internet*, Proceedings of the CSEE (in Chinese), vol. 38, no. 1, pp. 12–24+339 (2018).

[12] Liao Haizhu, Hu Haitao, Huang Yi *et al.*, *Day-ahead energy optimization and scheduling strategy of "source-network-train-storage" coordinated power supply system for electrified railways*, Electric Drive for Locomotives (in Chinese), no. 3, pp. 1–9 (2022), DOI: 10.13890/j.issn.1000-128X.2022.03.001.

[13] Qi Yan, Shang Junxue, Nie Jingyu *et al.*, *Optimization of CCHP micro-grid operation based on improved multi-objective grey wolf algorithm*, Electrical Measurement & Instrumentation (in Chinese), vol. 59, no. 6, pp. 12–19+52 (2022).

[14] Zhao Rui, Tan Zhongfu, Degejirifu U. *et al*., *Two-level coordinated operation optimization model of the source-storage-load in microgrid considering demand response*, Renewable Energy Resources (in Chinese), vol. 39, no. 16, pp. 4808–4818+4982 (2019).

[15] Song Wenqin, Lv Jinli, Zhao Linxia *et al*., *Study on the economic dispatch strategy of power system with combined operation of concentrated solar power and wind farm*, Power System Protection and Control (in Chinese), vol. 48, no. 5, pp. 95–102 (2020).

[16] Yang Zhipin, Li Kerun, Wang Ninglin *et al*., *Economic Analysis of Peaking Regulation of Coal-fired Generating Units Under Big Data*, Proceedings of the CSEE (in Chinese), vol. 44, no. 8, pp. 2754–2760 (2020).

[17] Lv Zhipeng, Lu Limin, Lu Huaigu *et al*., *Research on multi-mode energy management strategy of DC microgrid*, Distribution & Utilization (in Chinese), vol. 36, no. 7, pp. 44–51 (2019).

[18] Brahmendra Kumar V.G., Palanisamy K., *Energy management of renewable energy-based microgrid system with HESS for various operation modes*, Frontiers in Energy Research, vol. 10 (2022).

[19] Zhao Huirong, Mao Haifei, Peng Daogang, *Multi-object Nonlinear Economic Predictive Controller for Dynamic Energy Efficiency Optimization of MGT-LiBr CCHP Under Variable Working Conditions*, Proceedings of the CSEF (in Chinese), vol. 43, no. 8, pp. 3048–3059 (2023).

[20] Yu Xiaobo, Geng Yuqing, *Complementary Configuration Research of New Combined Cooling, Heating, and Power System Driven by Renewable Energy under Energy Management Modes*, Energy Technology, vol. 7, no. 10 (2019).

[21] Li Jiayuan, Li Yaonan, Hui Jilu, *Overview of Gray Wolf Algorithm Applications*, Digital Technology & Application Voltage Engineering (in Chinese), vol. 34, no. 5, pp. 963–972 (2019).

[22] Wang Zhi, Tao Hongjun, Cai Wenkui *et al*., *Optimal scheduling research of multi-time-scale-rolling optimization in CCHP system*, Acta Energiae Solar Sinica (in Chinese), vol. 44, no. 2, pp. 298–308 (2023).

[23] Kang Ligai, Yang Junhong, An Qingsong *et al*., *Complementary configuration and performance comparison of CCHP-ORC system with a ground source heat pump under three energy management modes*, Energy Conversion and Management, no. 135 (2017).

[24] Muhyaddin R., Abdullah A., Hussain B. *et al*., *Economical-technical-environmental operation of power networks with wind-solar-hydropower generation using analytic hierarchy process and improved grey wolf algorithm*, Ain Shams Engineering Journal, vol. 12, no. 3 (2021), DOI: 10.1016/j.asej.2021.02.004.

[25] Zhao Chao, Wang Bin, Sun Zhixin *et al*., *Optimal configuration optimization of islanded microgrid using improved grey wolf optimizer algorithm*, Acta Energiae Solar Sinica (in Chinese), vol. 43, no. 1, pp. 256–262 (2022).

[26] Mao Jingfeng, Wu Jian, Zhang Zhenmeng *et al*., *Multi-objective optimization of island-type DC microgrid based on AFPSO*, Acta Energiae Solar Sinica (in Chinese), vol. 42, no. 6, pp. 63–71 (2021).

[27] Farayi M., Alireza K., Mojtaba S.A. *et al*., *Multi-objective optimization of a biomass gasification to generate electricity and desalinated water using Grey Wolf Optimizer and artificial neural network*, Chemosphere, vol. 287, part 2 (2021), DOI: 10.1016/j.chemosphere.2021.131980.

[28] Gujarathi K.P., Shah A.V., Lokhande M.M., *Grey wolf algorithm for multidimensional engine optimization of converted plug-in hybrid electric vehicle*, Transportation Research Part D, vol. 63 (2018), DOI: org/10.1016/j.trd.2018.06.003.